

# Ion-image Interactions and Phase Transition at Electrolyte-Metal Interfaces

Alpha A. Lee<sup>\*,†</sup> and Susan Perkin<sup>‡</sup>

*School of Engineering and Applied Sciences, Harvard University, Cambridge, MA 02138, USA,  
and Department of Chemistry, Physical and Theoretical Chemistry Laboratory, University of  
Oxford, Oxford OX1 3QZ, U.K.*

E-mail: alphalee@g.harvard.edu

---

\*To whom correspondence should be addressed

†School of Engineering and Applied Sciences, Harvard University, Cambridge, MA 02138, USA

‡Department of Chemistry, Physical and Theoretical Chemistry Laboratory, University of Oxford, Oxford OX1 3QZ, U.K.

## Abstract

The arrangement of ions near a metallic electrode is crucial to energy storage in electrical double layer capacitors. Classic Poisson-Boltzmann theory predicts that the charge stored in the double layer is a continuous function of applied voltage. However, recent experiments and simulations strongly suggest the presence of a voltage-induced first order phase transition in the electrical double layer, leading to a hysteretic response — the capacitance-voltage relation is dependent on whether the voltage is increasing or decreasing. By developing a simple analytical model, we show that ion-image interaction could explain this phase transition. Moreover, our model shows that the presence of phase transition depends on the bulk energy of the ionic liquid. Our results justifies mixing ionic liquids with solvents as a way to achieve large capacitance and avoid hysteresis.

In recent years, electrical double layer capacitors (EDLCs) have received increasing attention because of their high power density and energy density.<sup>1-3</sup> In an EDLC, an ionic liquid or electrolyte solution is confined between two electrodes. In response to an applied voltage, ions accumulate near the oppositely charged electrode, and energy is stored across this electrified interface. As such, understanding the arrangement of ions near polarised surfaces is crucial to optimising EDLCs. The physics of ions near electrified interfaces is also crucial to modelling fuel cells and batteries, as well as other soft ionotronic devices such as polyelectrolyte electroactuators.<sup>4</sup>

The conventional wisdom, based on classic Gouy-Chapman-Stern mean field theory for dilute electrolytes,<sup>5</sup> predicts a densely packed layer of counterions near the electrode (the “Stern” layer) followed by an exponential decay in charge density (the “diffuse” layer). The charge stored in the double layer is predicted to be a continuous and monotonically increasing function of the applied voltage. Theories that incorporate effects of finite ion size<sup>6-10</sup> and electrostatic correlations<sup>7,11,12</sup> beyond the mean-field approximation have been developed. Despite qualitative differences in how the differential capacitance depends on the applied voltage, those models all predict a charge density which is a *continuous* function of applied voltage and thus the differential capacitance is *finite*. This phenomenology is also in agreement with a large body of experimental results and simulations.<sup>4</sup>

However, recent molecular dynamics simulations of ionic liquids (molten salts at room temperature) in contact with a polarised metallic electrode reveal the existence of a voltage-induced first order phase transition,<sup>13</sup> which is corroborated by experimental observation of structural transitions,<sup>14–18</sup> hysteresis<sup>17</sup> and anomalously large capacitance at the transition voltage<sup>15</sup> (for a review, see<sup>19</sup>). This novel phase transition has been rationalised in terms of non-electrostatic interactions that are prevalent in ionic liquids.<sup>20</sup> Those non-electrostatic interactions are believed to be important because ionic liquid cations and anions are of different sizes, and the alkyl chains on cations favour cation-cation packing. In fact, ionic liquids are comprised of domains of alkyl chains and domains of charged groups with locally heterogeneous dynamics<sup>21–23</sup> (for a recent review, see<sup>24</sup>). Using this physical picture, a recent theory based on a general Landau-Ginzburg expansion shows the possibility of a first order phase transition at finite applied voltage and a concomitant divergence in capacitance if one assumes that cations and anions will spontaneously demix if they were uncharged.<sup>20</sup> This pioneering theory provides a sufficient condition for phase transition at electrolyte-metal interfaces.

Nonetheless, although this recent theory reveals a possible mechanism that could drive phase transition, it raises the broader question of whether this transition is unique to ions with significant non-electrostatic interactions, and what role does the electrode material play in the transition. In this Letter, we argue that there is a confounding effect that drive phase transition — the ion-image interaction. The effect of ion-image interactions near a metallic surface has been explored in the literature on nanoporous supercapacitors and the physics of ions in confinement,<sup>25–28</sup> as well as the electrical double layer in ionic glasses.<sup>29</sup> We will apply a mean-field framework that has been successfully used for modelling nanoporous supercapacitors<sup>25,28</sup> to understand phase transition in the electrical double layer. Rather than providing quantitative results, the goal of our Letter is to present a heuristic argument of how ion-image interactions could drive the phase transition. As such, a simple but analytically tractable model will be used. Our main result is that non-electrostatic interactions are not necessary for the phase transition to occur — the reason why a phase transition is not observed for solutions of simple inorganic salt is merely because the salt

concentration is limited by solubility.

We will first review the two aspects of ion-image interactions in classic electrostatics: self-energy and interionic interactions.<sup>30</sup> An ion close to a metal surface induces an equal and opposite surface charge, the “image” charge, by polarising the electrons in the metal. As a result of this image charge, the self-energy of an ion is lower near a metal surface. Mathematically, an ion of charge  $+e$  located at distance  $d$  away from a metallic plate has self-energy,  $U_{\text{self}}$ , given by

$$\beta U_{\text{self}}(d) = -\frac{l_B}{2d}, \quad (1)$$

where  $\beta = 1/(k_B T)$  and  $l_B = e^2/(\epsilon k_B T)$  is the Bjerrum length with  $\epsilon$  the dielectric constant of the medium. Equation (1) has the physical interpretation of the ion interacting with an equal and opposite charge located at distance  $d$  behind the metal surface. Crucially, Equation (1) shows that it is thermodynamically favourable for an ion, regardless of the sign of its charge, to be as close to the metal surface as possible.

The second aspect of ion-image interactions is the concomitant weakening of interactions between neighbouring ions near a metallic surface. The ion-image couple behaves like a dipole, and the interaction between two like-charges located at distance  $d$  away from a metallic place and separated by distance  $r$  is given by

$$\beta U_{\text{dd}}(r) = \frac{l_B}{r} \left( 1 - \frac{1}{\sqrt{1 + (d/r)^2}} \right). \quad (2)$$

Equation (2) shows that the presence of a metallic surface weakens the long-ranged  $1/r$  Coulomb interaction in free space to a  $1/r^3$  dipolar interaction when  $r \gg d$ . Note that we have neglected effects of quantum capacitance and electric field penetration into the metal when we treat the electrode as an ideal metal,<sup>31</sup> which have been studied by quantum *ab initio* models.<sup>32,33</sup> Nonetheless, the physics that will be important for our model is the weakening of interionic interactions and a reduction in ion self-energy, which is a generic behaviour regardless of the approximation used to model the metal.

The weakening of ion-ion interaction near a metal surface, together with a favourable ion self-energy, suggest that the electrical double layer could be considered as comprising of two distinct parts even at zero applied voltage: a monolayer of ions adsorbed onto the metallic electrode surface, and a diffuse part away from the surface. In response to an applied voltage  $V$ , coions leave that monolayer, and counterions come in (Figure 1 shows a schematic sketch of our system). Note that this monolayer of ions is analogous but not the same as the Stern layer, as the latter is assumed to form only when  $eV/k_B T \gg 1$ .

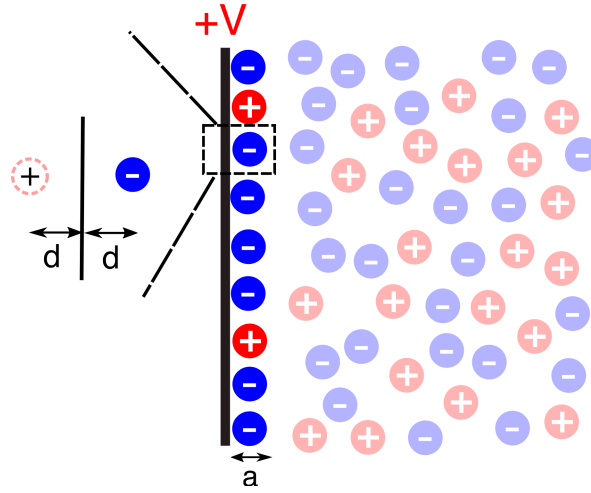


Figure 1: Charging of the electrical double layer. We focus on the monolayer of ions near the electrode to interrogate the role of ion-image interactions in driving phase transition. The zoomed-in box shows the ion-image analogy underlying Equations (1) and (2).

It is sufficient to only consider this monolayer of ion to see how ion-image interactions could lead to a phase transition; the idea of treating the interfacial region as distinct compared to the bulk has been applied to model counterion condensation.<sup>34,35</sup> We will make an additional simplifying assumption that the diffuse double layer and the bulk ionic liquid do not contribute to the screening of electrostatic interaction between the ions in the monolayer (our model uses the lower bound in the electrostatic screening). We consider a monolayer of ions of diameter  $a$  located at the distance of closest approach to the electrode surface. The free energy density of the monolayer with cation density  $\rho_+$  and anion density  $\rho_-$  is given by

$$\beta f(\rho_+, \rho_-) = E_{\text{el}}(\rho_+, \rho_-) + E_{\text{ent}}(\rho_+, \rho_-) + \mu_+ \rho_+ + \mu_- \rho_-, \quad (3)$$

where  $E_{\text{el}}$  is the electrostatic contribution,  $E_{\text{ent}}$  is the entropic contribution, and  $\mu_{\pm}$  is the electrochemical potential of the cation/anion. The electrostatic contribution can be estimated by<sup>25,28</sup>

$$\begin{aligned} E_{\text{el}} &= 2\pi c^2 \int_{R_c}^{\infty} \beta U_{\text{dd}}(r) r dr \\ &= 2\pi l_B c^2 \left( \sqrt{a^2 + R_c^2} - R_c \right), \end{aligned} \quad (4)$$

where  $R_c = 1/\sqrt{\pi\rho}$  is the mean separation between ionic species,  $c = \rho_+ - \rho_-$  is the charge density and  $\rho = \rho_+ + \rho_-$  is the total number density of ions. We model the entropic contribution with the lattice gas model which is often used in studying finite ion size effects in the electrical double layer,<sup>6,8,9</sup>

$$E_{\text{ent}} = (a^{-2} + \rho) \log(1 + a^2 \rho) + \sum_{\alpha=\pm} \rho_{\alpha} \log(a^2 \rho_{\alpha}). \quad (5)$$

Finally, the electrochemical potential of the cations and anions is given by

$$\mu_{\pm} = \pm \frac{eV}{k_B T} - \frac{l_B}{a} + \delta E_{\pm}, \quad (6)$$

where the first term is the interaction between the ions and the applied electric field, the second term is the self-energy term given by Equation (1), and the last term is the solvation energy of the ion in the bulk electrolyte. This last term is also known as ‘‘ionophobicity’’ in the context of nanoporous supercapacitors.<sup>27,28,36</sup> For a fixed applied voltage  $V$ , minimising the free energy (3) gives the equilibrium cation and anion densities. A first order phase transition is possible if the free energy has multiple minima, and hysteresis arises as the charging and discharging processes may follow different metastable branches of the free energy. We will use the `Matlab` routine `patternsearch` to search for local minima for a given  $V$ , and determine the global minimum from the local minima found.

To fix ideas, we will consider typical parameters for ionic liquids: ion diameter  $5\text{\AA}$ <sup>37</sup> and Bjerrum length  $l_B = 56\text{\AA}$  (corresponding to dielectric constant  $\epsilon = 10$  at room temperature<sup>38</sup>). We will consider cations and anions with the same resolution energy  $\delta E = \delta E_{\pm}$ . The resolution

energy  $\delta E$  is the free energy associated with desolvation as the ions lose roughly half of their solvation shell going from the bulk fluid to the electrode interface. However, the ions gain the image charge interaction when in the monolayer, together with any specific chemical or van der Waals interactions with the electrode. Therefore, we would expect that the transfer from the bulk to the electrode interface is roughly energetically neutral, i.e. the transfer energy  $\delta\mu = \delta E - l_B/a \approx 0$ . We note that for an electrolyte solution,  $\delta E$ , and thus  $\delta\mu$ , will be a function of concentration. In particular, we would expect  $\delta E$  to increase (i.e. the transfer from bulk to monolayer becomes less favourable) as the electrolyte is diluted with a high dielectric solvent. This is because a significant part of the solvation energy is the large entropy of ions in the dilute solution relative to monolayer confinement. In what follows, we will investigate the phenomenology predicted by our model for different values of  $\delta\mu$ , the transfer energy, close to zero.

We first consider the low voltage response of the system. A key quantity characterising the system is the differential capacitance

$$C_D = \frac{d\sigma}{dV}, \quad (7)$$

where  $\sigma$  is the charge (per area) of the monolayer. Figure 2 shows that the differential capacitance at zero voltage is a non-monotonic function of the transfer energy,  $\delta\mu$ . For large positive transfer energy, it is more energetically favourable for ions to reside in the bulk than the monolayer. Therefore, a small applied voltage does not lead to significant charging. In the opposite limit of large negative transfer energy, both co-ions and counterions are strongly adsorbed onto the electrode. Therefore, charging proceeds via swapping co-ions with counter-ions in a quid pro quo manner, and this swapping process needs to pay the energetic cost of increasing like-charge repulsion. In the intermediate regime with the transfer energy between the two extremes, the system charges by expelling co-ions but without increasing counterion concentration. This mitigates the like charge repulsion — from Equation (4), the electrostatic repulsion term can be kept constant by balancing the increase in charge density  $c$  with a decrease in total density  $\rho$ . Therefore, the system achieves the largest differential capacitance at zero applied voltage in this intermediate regime.

Experimentally, the transfer energy can be varied by adding solvent and diluting the ionic

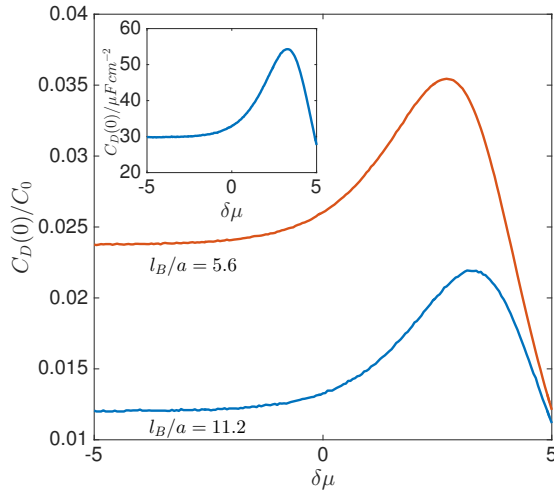


Figure 2: The capacitance at zero voltage is a non-monotonic function of the transfer energy,  $\delta\mu$ . The main panel shows the dimensionless capacitance, with  $C_0 = e^2/(k_B T a^2)$  setting the scale. The inset shows the dimensional capacitance plotted for  $l_B = 56\text{\AA}$  and  $a = 5\text{\AA}$ .

liquid. Our prediction, that there is a capacitance maximum at intermediate dilution ( $\delta\mu$ ), is in agreement with recent experimental results.<sup>39</sup> The inset of Figure 2 shows the capacitance in dimensional units; the capacitance maximum predicted by our simple model ( $\approx 50\mu\text{Fcm}^{-2}$ ) is comparable to experimental results ( $\approx 25\mu\text{Fcm}^{-2}$ ).

We now turn to the possibility of a voltage-induced phase transition. Figures 3(a)-(b) show the charging mechanism for different values of the transfer energy. For large, positive, transfer energy, the total ion density in the monolayer is low at zero applied voltage. Counterion adsorption is driven by the applied voltage, and charging is a continuous process. The monolayer becomes increasingly packed with ions as the transfer energy decreases, and charging proceeds via expelling co-ions first before counterions adoption to offset the penalty of like-charge repulsion. Therefore, at low applied voltages, the total ion density in the monolayer decreases whilst the charge density increases. Finally, when the transfer energy falls below a threshold, the expulsion of co-ions is discontinuous, and thus the concomitant increase in charge density is also discontinuous. This discontinuous increase in charge density leads to a divergence in the differential capacitance.

The physics of this phase transition is further illustrated by the energy landscape at the transition voltage, Figure 3(c). There are two distinct and iso-energetic ways to arrange the system at the

transition voltage — high co-ion density, which is favoured by electrostatics and transfer energy, or low co-ion density, which is favoured by the applied potential. Below the transition voltage, electrostatics and transfer energy dominates and thus the co-ion rich state is favourable, and beyond the transition voltage the effect of the applied voltage dominates and the co-ion deficient state is favourable. The transition voltage increases as the transfer energy becomes more negative, as seen in Figure 3(d). However, phase transition disappears for transfer energies beyond the critical endpoint (the dot in Figure 3(d)). Beyond the critical endpoint, the monolayer is loosely packed to start with and thus there are not many co-ions to expel.

As the phase transition is first order, the charging and discharging paths may follow different metastable states. This introduces the possibility of hysteresis, as observed in experiments. Hysteresis, in turn, will lead to energy losses, making the capacitor less efficient. Nonetheless, our model identifies a remedy for hysteresis — phase transition and hysteresis are absent as long as the transfer energy is above the critical endpoint (Figure 3(d)). This can be achieved by diluting the ionic liquid, for example. In fact, the capacitance maximum in Figure 2 is beyond the critical endpoint of phase transition. This suggests that using an ionic liquid-solvent mixture as the electrolyte maximises capacitance as well as avoids hysteresis.

The existence of a critical endpoint in Figure 3(d) also sheds light on why this phase transition has not been observed for solutions of simple inorganic salts. Finite solubility of such salts means that the  $\delta\mu$  may never venture beyond the critical endpoint. As such, our model suggests that the reason why this phase transition has, so far, been observed in ionic liquids only is not necessarily due to ionic liquid-specific forces between ions. It is simply because ionic liquids are liquids, which in turn is because ionic liquid ions are large and geometrically difficult to pack into a crystalline lattice.<sup>40</sup> A similar phase transition is expected for molten inorganic salts, although its very high melting temperature is a barrier to experimental investigation.

In deriving our model, Equation (3), we have made several assumptions which we will now comment on. First, our free energy takes the ion densities as order parameters. While justified for transitions that preserves the symmetry of the system (liquid/vapour type), it may not capture

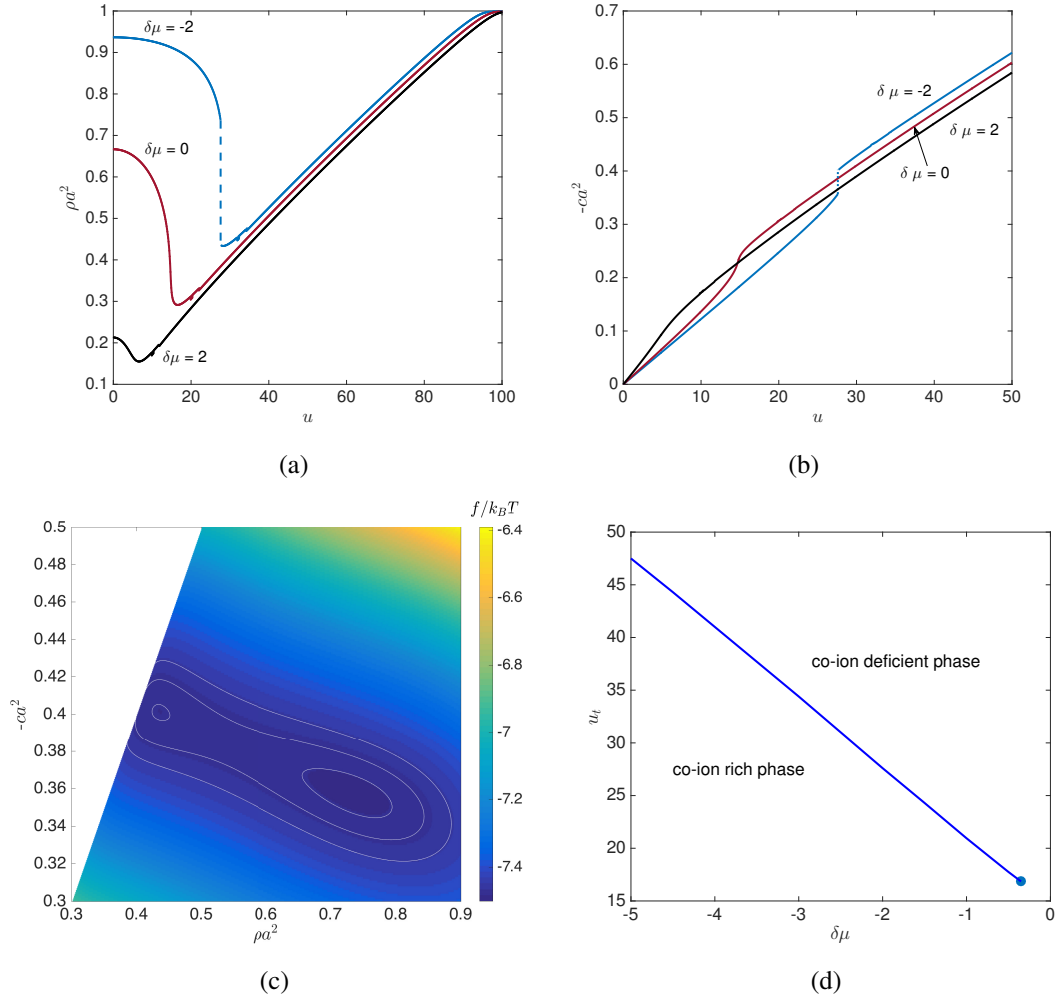


Figure 3: Voltage-induced phase transition is predicted for transfer energy  $\delta\mu$  below a threshold. The total density (a) and charge density (b) as a function of dimensionless applied potential  $u = \beta eV$  display discontinuity at the transition voltage. (c) The free energy landscape at the transition voltage shows two degenerate energy minima corresponding to co-ion rich and co-ion poor phases. The white contour lines show the location of the free energy basins. Note that a portion of phase space is excluded because of steric constraints. (d) The phase diagram of the transition showing the transition voltage  $u_t$  as a function of the transfer energy  $\delta\mu$ , with the dot indicating the critical endpoint. The figures are plotted for  $l_B = 56\text{\AA}$  and  $a = 5\text{\AA}$ .

liquid/solid-like transition and the complex patterns formed on electrodes.<sup>19</sup> However, understanding the possibility of symmetry-preserving transitions is crucial before investigating symmetry-breaking ones. Second, we have ignored the non-electrostatic like-charge interactions which is the focus of.<sup>20</sup> Our goal is to show that phase transition is possible even without non-electrostatic interactions. Moreover, dilution with polar solvent will likely disrupt the microstructures in neat ionic

liquids and render ionic liquid solution similar to solutions of inorganic salts. Finally, we have treated the transfer energy  $\delta\mu$  as a phenomenological parameter. Although the precise functional dependence of  $\delta\mu$  on the electrolyte concentration depends on the chemistry of the solvent and ions, which will be considered in future works, the key insights given by our model rely only on the generic observation that  $\delta\mu$  becomes more negative as the electrolyte concentration increases.

In summary, we have shown that ion-image interactions explain the capacitive behaviour of ionic liquid-solvent mixtures and the phenomenology of phase transition observed at electrolyte-metal interfaces. We identify the transfer energy, tunable via dilution, as a key parameter that determines the capacitance as well as the presence of phase transition. Our results demonstrate how “doping” ionic liquids with solvents act to significantly enhance the performance of electrical double layer capacitors. Systematic experimental studies on using ionic liquid-solvent mixtures in electrical double layer capacitors are currently scarce, and we hope that our theory will provide a framework to assess and direct future efforts to address this.

## Acknowledgement

AAL is supported by a UK-US Fulbright Fellowship to Harvard University. SP is supported by The Leverhulme Trust (RPG- 380 2015-328), the ERC (under Starting Grant LIQUISWITCH), and The John Fell Fund (Oxford University).

## References

- (1) Simon, P.; Gogotsi, Y. Materials for Electrochemical Capacitors. *Nat. Mater.* **2008**, *7*, 845–854.
- (2) Miller, J. R.; Simon, P. Electrochemical Capacitors for Energy Management. *Science* **2008**, *321*, 651–652.
- (3) Conway, B. E. *Electrochemical Supercapacitors: Scientific Fundamentals and Technological Applications*; Springer Science & Business Media, 2013.

- (4) Fedorov, M. V.; Kornyshev, A. A. Ionic Liquids at Electrified Interfaces. *Chem. Rev.* **2014**, *114*, 2978–3036.
- (5) Parsons, R. The Electrical Double Layer: Recent Experimental and Theoretical Developments. *Chem. Rev.* **1990**, *90*, 813–826.
- (6) Bikerman, J. XXXIX. Structure and Capacity of Electrical Double Layer. *Lond. Edinb. Dubl. Phil. Mag.* **1942**, *33*, 384–397.
- (7) Attard, P. Electrolytes and the Electric Double Layer. *Adv. Chem. Phys.* **1996**, *92*, 1–160.
- (8) Borukhov, I.; Andelman, D.; Orland, H. Steric Effects in Electrolytes: A Modified Poisson-Boltzmann Equation. *Phys. Rev. Lett.* **1997**, *79*, 435.
- (9) Kornyshev, A. A. Double-Layer in Ionic Liquids: Paradigm Change? *J. Phys. Chem. B* **2007**, *111*, 5545–5557.
- (10) Frydel, D.; Levin, Y. A Close Look into the Excluded Volume Effects Within a Double Layer. *J. Chem. Phys.* **2012**, *137*, 164703.
- (11) Bazant, M. Z.; Storey, B. D.; Kornyshev, A. A. Double Layer in Ionic Liquids: Overscreening versus Crowding. *Phys. Rev. Lett.* **2011**, *106*, 046102.
- (12) Lee, A. A.; Kondrat, S.; Vella, D.; Goriely, A. Dynamics of Ion Transport in Ionic Liquids. *Phys. Rev. Lett.* **2015**, *115*, 106101.
- (13) Merlet, C.; Limmer, D. T.; Salanne, M.; Van Roij, R.; Madden, P. A.; Chandler, D.; Rotenberg, B. The Electric Double Layer has a Life of Its Own. *J. Phys. Chem. C* **2014**, *118*, 18291–18298.
- (14) Pan, G.-B.; Freyland, W. 2D Phase Transition of PF<sub>6</sub> Adlayers at the Electrified Ionic Liquid/Au (111) Interface. *Chem. Phys. Lett.* **2006**, *427*, 96–100.

- (15) Su, Y.-Z.; Fu, Y.-C.; Yan, J.-W.; Chen, Z.-B.; Mao, B.-W. Double Layer of Au (100)/Ionic Liquid Interface and Its Stability in Imidazolium-Based Ionic Liquids. *Angew. Chem. Int. Ed.* **2009**, *121*, 5250–5253.
- (16) Uysal, A.; Zhou, H.; Feng, G.; Lee, S. S.; Li, S.; Fenter, P.; Cummings, P. T.; Fulvio, P. F.; Dai, S.; McDonough, J. K.; Gogotsi, Y. Structural Origins of Potential Dependent Hysteresis at the Electrified Graphene/Ionic Liquid Interface. *J. Phys. Chem. C* **2013**, *118*, 569–574.
- (17) Uysal, A.; Zhou, H.; Feng, G.; Lee, S. S.; Li, S.; Cummings, P. T.; Fulvio, P. F.; Dai, S.; McDonough, J. K.; Gogotsi, Y. Interfacial Ionic “Liquids”: Connecting Static and Dynamic Structures. *J. Phys.: Condens. Matter* **2014**, *27*, 032101.
- (18) Wen, R.; Rahn, B.; Magnussen, O. M. Potential-Dependent Adlayer Structure and Dynamics at the Ionic Liquid/Au (111) Interface: A Molecular-Scale In Situ Video-STM Study. *Angew. Chem. Int. Ed.* **2015**, *54*, 6062–6066.
- (19) Rotenberg, B.; Salanne, M. Structural Transitions at Ionic Liquid Interfaces. *J. Phys. Chem. Lett.* **2015**, *6*, 4978–4985.
- (20) Limmer, D. T. Interfacial Ordering and Accompanying Divergent Capacitance at Ionic Liquid-Metal Interfaces. *Phys. Rev. Lett.* **2015**, *115*, 256102.
- (21) Del Pópolo, M. G.; Voth, G. A. On the Structure and Dynamics of Ionic Liquids. *J. Phys. Chem. B* **2004**, *108*, 1744–1752.
- (22) Wang, Y.; Voth, G. A. Unique Spatial Heterogeneity in Ionic Liquids. *J. Am. Chem. Soc.* **2005**, *127*, 12192–12193.
- (23) Hu, Z.; Margulis, C. J. Heterogeneity in a Room-Temperature Ionic Liquid: Persistent Local Environments and the Red-Edge Effect. *Proc. Natl. Acad. Sci. USA* **2006**, *103*, 831–836.
- (24) Hayes, R.; Warr, G. G.; Atkin, R. Structure and Nanostructure in Ionic Liquids. *Chem. Rev.* **2015**, *115*, 6357–6426.

- (25) Kondrat, S.; Kornyshev, A. A. Superionic State in Double-Layer Capacitors with Nanoporous Electrodes. *J. Phys.: Condens. Matter* **2010**, *23*, 022201.
- (26) Skinner, B.; Chen, T.; Loth, M. S.; Shklovskii, B. I. Theory of Volumetric Capacitance of an Electric Double-Layer Supercapacitor. *Phys. Rev. E* **2011**, *83*, 056102.
- (27) Lee, A. A.; Kondrat, S.; Kornyshev, A. A. Single-File Charge Storage in Conducting Nanopores. *Phys. Rev. Lett.* **2014**, *113*, 048701.
- (28) Lee, A. A.; Vella, D.; Goriely, A.; Kondrat, S. Capacitance-Power-Hysteresis Trilemma in Nanoporous Supercapacitors. *Phys. Rev. X* **2016**, *6*, 21034.
- (29) Skinner, B.; Loth, M. S.; Shklovskii, B. I. Capacitance of the Double Layer Formed at the Metal/Ionic-Conductor Interface: How Large Can It Be? *Phys. Rev. Lett.* **2010**, *104*, 128302.
- (30) Jackson, J. D. *Classical Electrodynamics*; Wiley, 1999.
- (31) Schmickler, W.; Henderson, D. New Models for the Structure of the Electrochemical Interface. *Prog. Surf. Sci.* **1986**, *22*, 323–419.
- (32) Spohr, E. Some Recent Trends in Computer Simulations of Aqueous Double Layers. *Electrochim. Acta* **2003**, *49*, 23–27.
- (33) Luque, N. B.; Woelki, S.; Henderson, D.; Schmickler, W. A Model for the Electrical Double Layer Combining Integral Equation Techniques with Quantum Density Functional Theory. *Electrochim. Acta* **2011**, *56*, 7298–7302.
- (34) Lau, A. W. C.; Lukatsky, D. B.; Pincus, P.; Safran, S. A. Charge Fluctuations and Counterion Condensation. *Phys. Rev. E* **2002**, *65*, 051502.
- (35) Lau, A. W. C.; Pincus, P. Counterion Condensation and Fluctuation-Induced Attraction. *Phys. Rev. E* **2002**, *66*, 041501.

- (36) Forse, A. C.; Merlet, C.; Griffin, J. M.; Grey, C. P. New Perspectives on the Charging Mechanisms of Supercapacitors. *J. Am. Chem. Soc.* **2016**,
- (37) Perkin, S.; Crowhurst, L.; Niedermeyer, H.; Welton, T.; Smith, A. M.; Gosvami, N. N. Self-Assembly in the Electrical Double Layer of Ionic Liquids. *Chem. Commun.* **2011**, *47*, 6572–6574.
- (38) Huang, M.-M.; Jiang, Y.; Sasisanker, P.; Driver, G. W.; Weingärtner, H. Static Relative Dielectric Permittivities of Ionic Liquids at 25 C. *J. Chem. Eng. Data* **2011**, *56*, 1494–1499.
- (39) Bozym, D. J.; Uralcan, B. I.; Limmer, D. T.; Pope, M. A.; Szamreta, N. J.; Debenedetti, P. G.; Aksay, I. A. Anomalous Capacitance Maximum of the Glassy Carbon–Ionic Liquid Interface through Dilution with Organic Solvents. *J. Phys. Chem. Lett.* **2015**, *6*, 2644–2648.
- (40) Krossing, I.; Slattery, J. M.; Daguene, C.; Dyson, P. J.; Oleinikova, A.; Weingärtner, H. Why are Ionic Liquids Liquid? A Simple Explanation Based on Lattice and Solvation Energies. *J. Am. Chem. Soc.* **2006**, *128*, 13427–13434.

## Graphical TOC Entry

